Mn-Zn Ferrite Nanoparticles with Silica and Titania Coatings: Synthesis, Transverse Relaxivity and Cytotoxicity

Ondřej Kaman[1], Jarmila Kuličková[1], Miroslav Maryško[1], Pavel Veverka[1], Vít Herynek[2], Radim Havelek[3], Karel Královec[4], Denisa Kubániová[5], Jaroslav Kohout[5], Petr Dvořák[5], and Zdeněk Jirák[1]

[1] Institute of Physics of the Czech Academy of Sciences, 162 00 Praha 6, Czech Republic
[2] Institute for Clinical and Experimental Medicine, 140 21 Praha 4, Czech Republic
[3] Faculty of Medicine in Hradec Kralove, Charles University, 500 03 Hradec Králové, Czech Republic
[4] Faculty of Chemical Technology, University of Pardubice, 532 10 Pardubice, Czech Republic
[5] Faculty of Mathematics and Physics, Charles University, 180 00 Praha 8, Czech Republic

Mn-Zn ferrite nanoparticles of the composition $Mn_{0.61}Zn_{0.42}Fe_{1.97}O_4$ and mean size of crystallites d_{XRD} = 11 nm are synthesized under hydrothermal conditions as a single-phase product. Subsequently, two coated samples are prepared by encapsulation of the ferrite particles into silica and titania. Transmission electron microscopy confirms the core-shell structure of the products and shows that the cores are actually formed by small clusters of ferrite crystallites. Powder X-ray diffraction combined with experimental hydrothermal treatment of the titania-coated product demonstrates that the titania coating is amorphous but can be easily transformed to anatase. The colloidal stability of nanoparticles in water is evidenced by dynamic light scattering, and the respective hydrodynamic sizes are d_Z = 87 nm and 157 nm for silica-coated and titania-coated particles. The colloidal behavior is confirmed based on the measurements of zeta-potential, whose negative values lead to strong Coulombic repulsion among coated particles. Magnetic measurements on bare and coated particles show high magnetization of $Mn_{0.61}Zn_{0.42}Fe_{1.97}O_4$ cores and superparamagnetic state at room temperature. The relaxometric study on aqueous suspensions in magnetic fields of 0.5 T and 11.75 T reveals high transverse relaxivity of the samples and two distinct forms of its temperature dependence, which are analyzed with respect to the role of temperature-dependent parameters, i.e., the diffusion of water and the magnetization of ferrite cores. Finally, careful evaluation of cytotoxicity of coated particles is carried out by using two different methods, namely the determination of viability and proliferation of Jurkat cells and the real-time monitoring of attachment and proliferation of A549 cells. In the studied range of concentrations, the viability and proliferation of suspension cells are not affected, and only negligible effects are detected in the cell index of adherent cells.

Index Terms—**Amorphous titania, silica, magnetic nanoparticles, Mn-Zn ferrite, transverse relaxivity, cytotoxicity.**

I. INTRODUCTION

MAGNETIC NANOPARTICLES with hydrophilic coatings have been a subject of intense research with respect to medical applications for long time. A plethora of concepts have been suggested for new diagnostic and therapeutic methods, whose integration into a single approach, i.e., theranostics seems to be not only an attractive goal of medical research but already a feasible option. The nanoscale dimensions of magnetic particles and availability of efficient procedures for their functionalization provide necessary tools for efficient preparation of complex nanosystems. Theranostic nanoparticles with magnetic cores could serve as contrast agents for MRI (magnetic resonance imaging), labeling agents for exceptionally sensitive MPI (magnetic particle imaging), heating mediators for magnetic hyperthermia, and advanced drug delivery systems with magnetically triggered effects [1]. However, such advanced applications are usually accompanied by specific requirements on magnetic behavior of the particles, and high magnetization is not the only desired attribute. The possibility of tuning the magnetic anisotropy of particles in broad range, the precise adjustment of the critical temperature for transition to paramagnetic state, or just a marked temperature dependence of their magnetic properties on temperature enable optimization for a particular application and offer even new options, such as self-regulated hyperthermia [2] or development of temperature sensors [3].

Simple iron oxides represent a traditional choice due to their low toxicity, ease of preparation, and extensive knowledge of their properties and biological fate but their magnetic behavior can be altered only in a limited way by virtue of the size and shape of particles. In contrast, magnetic properties of ferrite nanoparticles can be easily adjusted in a broad range by their chemical composition, i.e., by selection of a convenient parent compound and suitable doping. Moreover, the doping of these ferrimagnetically ordered structures by a diamagnetic cation with particular preference for tetrahedral sublattice increases the net magnetic moment of the compound. The Mn-Zn ferrite of the composition close to $Mn_{0.6}Zn_{0.4}Fe_2O_4$, showing the highest magnetization in the $Mn_{1-x}Zn_xFe_2O_4$ system, is an excellent example [4].

As the hydrophilic coatings are concerned, amorphous silica, providing biologically inert surface and stable barrier around magnetic cores, is a commonly applied material, and a variety of procedures employing the Stöber process have been developed to encapsulate diverse nanoparticles into silica [5], [6]. However, certain inorganic materials whose deposition is not so facile show the same advantages as silica and, in addition, might be useful for theranostic applications on its own. The particularly attractive material is titania [7], the electronic structure of which leads to strong photocatalytic activity. The electron-hole pairs induced upon irradiation react

with O_2 molecules, while reactive oxygen species, such as •OH, O_2^-, and H_2O_2, are formed [8]. These species can be used for highly localized photodynamic therapy of cancer.

The present study aims to employ $Mn_{0.6}Zn_{0.4}Fe_2O_4$ ferrite nanoparticles as magnetic cores with high magnetization and coat them with two distinct types of coatings, namely silica and titania. The detailed characterizations of the corresponding products will focus on their morphology, size, and colloidal behavior along with the magnetic properties. In the following part, their transverse relaxivity, which is as a crucial parameter for MRI, will be evaluated, and its temperature dependence will be analyzed. Finally, biological effects of the coated particles will be studied *in vitro*.

II. EXPERIMENTAL DETAILS

A. Preparation of Samples

Mn-Zn ferrite nanoparticles (MZF) were synthesized under hydrothermal conditions strictly according to the previously described procedure [9]. The molar ratio of Mn : Zn : Fe employed for the present sample was 0.60 : 0.40 : 1.80 with intentionally substechiometric amount of iron to prevent occurrence of hematite as an impurity in the product.

The silica-coated sample (MZF@silica) was prepared by stabilization of Mn-Zn ferrite nanoparticles by citrate and their subsequent encapsulation into silica as follows. At first, the MZF particles (150 mg) were dispersed in ice-cold 1 M nitric acid and treated by ultrasound for 15 min. After separation by centrifugation, the particles were treated in the same way by ice-cold 0.1 M citric acid. One washing cycle in water followed, and the particles were redispersed in water (20 mL) alkalized with few drops of ammonia by means of an ultrasound probe. The stable suspension was transferred into the mixture of ethanol (340 mL of the azeotrope), water (70 mL), and ammonia (22 mL) in 0.5 L round bottom flask, which was equipped by a Teflon mechanical stirrer and was placed in an ultrasound bath stabilized at 60 °C. While both the mechanical and ultrasound agitation was applied, tetraethoxysilane (4.38 mL) was added. The ultrasound agitation was terminated soon after the addition, and the heating was ended after 4 h. The mechanical stirring continued overnight. The raw coated particles were separated and thoroughly washed with ethanol and water. Size fractionation was carried out by repeated differential centrifugation at 1,860 rcf for 15 min in three cycles, during which the supernatant was collected, and the residue was recycled for a following cycle. Finally, the combined supernatants were fractionated again at 1,860 rcf for 15 min.

The titania-coated particles (MZF@TiO$_2$) were obtained by stabilization of Mn-Zn ferrite nanoparticles by a cationic surfactant followed by a coating procedure under high dilution conditions. Specifically, MZF particles (30 mg) were intensively dispersed in 0.15 wt% aqueous solution (20 mL) of cetyltrimethylammonium bromide (CTAB) by a probe-type ultrasonicator for 4 h. The suspension was diluted by methanol (80 mL), and the mixture, placed in a 0.5 L round bottom flask, was agitated mechanically and by ultrasound for additional 0.5

h. Then, the continuous addition (0.11 mL·min^{-1}) of titanium butoxide (200 μL) solution in absolute ethanol (20 mL) was started. The mixture was stirred overnight, and the raw product was separated by centrifugation. Thorough washing with ethanol and water followed. Thereafter, simple size fractionation, consisting in a single differential centrifugation at 1,860 rcf for 15 min, was applied.

The residue separated from the final MZF@TiO$_2$ product by centrifugation was employed for powder X-ray diffraction (XRD) and was also subjected to experimental hydrothermal treatment in pure water at 200 °C for 12 h to study the crystallization of titania.

B. Fundamental Characterizations

The phase composition, crystal structure, and mean size of crystallites were studied by XRD with CuKα radiation. The XRD patterns were collected on a Bruker D8 diffractometer and were analyzed by the Rietveld method in the FULLPROF program. The d_{XRD} values were evaluated based on peak broadening, for which the Thompson-Cox-Hastings pseudo-Voigt profile was applied to separate the size and strain contribution, whereas the instrumental profile was determined on a strain-free tungsten powder with crystallite size of 9.4 μm.

The chemical composition of the bare ferrite cores was determined by means of X-ray fluorescence spectroscopy (XRF) carried out on an Axios spectrometer. The concentration of ferrite particles in aqueous suspensions was determined through analysis of iron by atomic absorption spectroscopy with flame atomization at $\lambda = 248.3$ nm. The samples were prepared by chemical digestion with HF and HNO_3, and small amount of H_2O_2 was added to reduce all manganese to Mn^{2+}. The final solution for the AAS measurement was based on 1.3% HNO_3 in the case of MZF@silica and 0.13% HF in the case of MZF@TiO$_2$. The standard addition method was applied to rule out any matrix effects, and the analysis was performed in triplicates.

Transmission electron microscopy (TEM) was carried out on Philips CM 120 to analyze the morphology and size of particles. The colloidal stability and hydrodynamic size of coated particles in water at 25 °C were probed by dynamic light scattering (DLS) that was measured on Malvern Zetasizer Nano S. The same instrumentation was used also for laser Doppler electrophoresis to measure the zeta potential of particles in aqueous suspensions.

Magnetic properties of bare and coated particles were studied by SQUID magnetometry by using a Quantum Design MPMS XL system. Before the measurements, the coated samples were subjected to an identical drying procedure at 105 °C under normal pressure. Careful demagnetization of the magnet was carried out prior to the zero-field-cooled/field-cooled (ZFC/FC) measurements.

C. Relaxometry

Dilute aqueous suspensions of both types of coated particles were used for relaxometric studies in the magnetic fields of B_0 = 0.5 T (Bruker Minispec relaxometer) and 11.75 T (Bruker Avance III HD 500 MHz spectrometer). The transverse

relaxation time in a given field was measured as a function of temperature, which was controlled by an external water bath and probed directly in the suspension for the measurement at 0.5 T, whereas heated airflow and thermocouple in close contact with sample were used at 11.75 T. A modified CPMG multi-echo sequence was employed. The following parameters were applied for the measurement at 0.5 T: 1,000 echoes, echo spacing of 2 ms, recovery time TR = 5,000 ms, number of acquisitions AQ = 4, and 2 dummy scans. For the measurement at 11.75 T, the number of echoes and echo spacing was set depending on the experiment, echo spacing equaled 0.42 ms, TR = 8,000–50,000 ms, AQ = 8, and 16 points in total were used to determine the transverse relaxation time T_2.

D. Evaluation of Cytotoxicity of Coated Nanoparticles

The human lung carcinoma cell line A549 (p53 wild-type) and human leukemic T-cell lymphoblast cell line Jurkat (p53-deficient) were obtained from the European Collection of Cell Cultures and were propagated under conditions specified in [10].

The real-time monitoring of growth and adherent properties of A549 cells treated with coated nanoparticles was performed by using an xCELLigence system. The exact procedure followed the details described in the previous study [10]. Approximately 24 h after seeding, when the log growth phase was achieved, the cells were exposed in tetraplicates to 10 µL of sterile deionized water with the tested nanoparticles to obtain final concentrations of 0.035–0.14 mmol(Me₃O₄)·L⁻¹ and 0.018–0.070 mmol(Me₃O₄)·L⁻¹ for MZF@silica and MZF@TiO₂ nanoparticles, respectively. Negative controls received sterile deionized water for cell cultures, whereas cells treated with 5% DMSO were used as positive control.

The effect of coated nanoparticles on proliferation and viability of Jurkat cells was studied by the trypan blue exclusion test. The cells were seeded at the concentration of 2×10^5 cells/mL and were treated with coated nanoparticles at three different concentrations, namely 0.035, 0.070, 0.14 mmol(Me₃O₄)·L⁻¹ for MZF@silica and 0.018, 0.035, 0.070 mmol(Me₃O₄)·L⁻¹ for MZF@TiO₂. Further, cells treated with doxorubicin at 0.25 µmol·L⁻¹ were used as a positive control. All experiments were carried out in triplicates. The cell proliferation and viability were determined 24 and 48 h following the treatment by examining the cell membrane integrity through the trypan blue exclusion technique. Specifically, 50 µL of 0.4% trypan blue was mixed with 50 µL of cell suspension, and the live and dead cells were counted in a Bürker chamber. The results were expressed as arithmetic means with standard deviations, and the null hypothesis that the means are equal to the mean of the negative control was tested by using unpaired t test, whereas the alternative hypothesis assumed that the mean of the control is higher.

III. RESULTS AND DISCUSSION

A. Structure, Morphology and Colloidal Properties

The XRD analysis of bare MZF particles evidenced the single-phase character of the sample with no signs of hematite or hausmannite phases as admixtures. The spinel structure of the $Fd\bar{3}m$ symmetry was confirmed, and the cubic lattice parameter was refined to a = 8.4576(4) Å. The XRD pattern, depicted in Fig. 1, was characterized by considerable peak broadening, on the basis of which the mean crystallite size of d_{XRD} = 11 nm was evaluated. The chemical composition of bare particles was determined by XRF to be Mn₀.₆₂Zn₀.₄₁Fe₁.₉₇O₄, which closely corresponds to the initial ratio of Mn : Zn employed for the synthesis.

The XRD pattern of the titania-coated product showed that the titania was amorphous since no other crystalline phases than the Mn-Zn ferrite were observed. However, the additional hydrothermal treatment of the as-prepared MZF@TiO₂ particles at 200 °C (see Fig. 1 for the XRD patterns of the as-prepared and hydrothermally treated samples) demonstrated that the amorphous titania shell could be easily transformed to anatase, i.e., the most active phase among TiO₂ polymorphs with respect to photocatalytic properties [7].

FIG. 1 HERE

Representative transmission electron micrographs of the citrate-stabilized bare cores and both the coated products are shown in Fig. 2a-c. Considering that the mean size of crystallites evaluated from XRD is a volume-weighted average, the d_{XRD} value is in excellent agreement with the size of ferrite nanoparticles according to TEM (*vide infra*), which implies that the mostly spherical ferrite particles observable in Fig. 2a are individual crystallites.

In the MZF@silica product, the ferrite crystallites form small clusters that are coated as a whole by silica shell. The detailed image analysis of the silica-coated particles confirms this observation by conclusive data. In a spherical approximation, the size of individual ferrite nanoparticles distinguishable within the coated clusters is described by a lognormal distribution with the arithmetic mean of $\bar{d}_i$ = 10 nm and the arithmetic standard deviation of sd_i = 2 nm, whereas the corresponding volume-weighted mean is $\bar{d}_{i,vw}$ = 11 nm. Whole magnetic cores formed by the mentioned clusters are characterized by a lognormal distribution with the arithmetic mean of $\bar{d}_c$ = 26 nm and sd_c = 7 nm (the volume-weighted mean is $\bar{d}_{c,vw}$ = 31 nm). Considering the given arithmetic means and the packing factor of the most dense arrangement of spheres, i.e. 74%, an average magnetic core of MZF@silica particles is formed by a cluster of 13 ferrite nanoparticles. The diameter of the whole silica-coated particles is also lognormally distributed with the arithmetic mean and arithmetic standard deviation of $\bar{d}_p$ = 65 nm and sd_p = 9 nm, respectively, (the volume-weighted mean is $\bar{d}_{p,vw}$ = 68 nm). Further, the silica shell of these particles is very uniform with only limited variation in the thickness, whose average value is 19 nm with standard deviation of 1 nm, and the shell exhibits smooth surface.

The rigorous image analysis of MZF@TiO₂ was not so straightforward as for the silica-coated sample taking into

account lower contrast between ferrite cores and titania shell and more complex morphology of the titania-coated product. Nevertheless, it is obvious that the mean size of MZF@TiO$_2$ particles is larger and the titania-coated clusters partially merge into larger formations. Further, the titania shell is very coarse, and the thickness of the shell varies considerably from the first nanometers to roughly 20 nm.

FIG. 2 HERE

The morphological peculiarities of the MZF@TiO$_2$ product originated in the distinct coating procedure that had to be applied. Actually, the kinetics of hydrolysis and polycondensation of titanium alkoxides is much faster compared to the reaction of their silicon counterparts [11]. And such reactivity complicates the preparation of well-defined core-shell particles since immediate precipitation of free titania usually occurs instead of its deposition on the surface of particles. In order to decrease the probability of nucleation of pure titania, the coating procedure was performed under high-dilution conditions achieved by the continuous addition of a dilute solution of the titanium butoxide, that immediately reacted. In addition, the cationic surfactant CTAB was used for the stabilization and surface modification of bare cores to increase their affinity to titania, which shows a negative zeta-potential [12]. Actually, preliminary experiments on the deposition of titania on MZF cores stabilized by citrate were not successful. Nevertheless, considering that CTAB is used as a typical template for preparation of mesoporous materials [13], [14], the as-prepared titania coating may be highly porous. And the detailed TEM analysis of MZF@TiO$_2$ particles at large magnification revealed certain patterns on titania shells that might be a signature of its mesoporous structure.

The distribution of hydrodynamic sizes, evaluated from the DLS measurements, confirms the larger size of MZF@TiO$_2$ particles (see Fig. 2d). Specifically, the Z-average values of d_Z = 87 nm and 157 nm and polydispersity indices of pdi = 0.065 and 0.072 are determined for MZF@silica and MZF@TiO$_2$ nanoparticles, respectively. More importantly, the DLS study evidences the colloidal stability of both the products in water, which is further supported by zeta potential measurements under neutral pH. The latter study proves strong Coulombic repulsion among coated nanoparticles as the zeta potential values of -40 mV and -35 mV are observed for the MZF@silica and MZF@TiO$_2$ samples.

B. Magnetic Properties

The hysteresis loops for the bare Mn-Zn ferrite cores and the coated products at low and room temperatures are depicted in Fig. 3. The specific magnetization of bare cores reaches high values of $M(5K)$ = 112 Am^2·kg^{-1} and $M(300K)$ = 57 Am^2·kg^{-1} in the magnetic field of 3 T, and the magnetic moment of spontaneous ordering at 5 K, evaluated by an extrapolation of the magnetization to zero field, is 4.55 μ_B per formula unit. At room temperature, the magnetization drops to $M(300K)$ = 57 Am^2·kg^{-1}, which agrees well with the previous report on Mn-Zn ferrite nanoparticles of similar composition and size [15], and reflects the approaching of Curie temperature at about 550 K.

The specific magnetization of coated products is considerably lower compared to the specific magnetization of the bare sample because of the large weight content of diamagnetic components. The ratio of the respective values of magnetization, in a rough approximation corresponding to the weight content of the ferrite phase, is 9% for the MZF@silica sample and 29% for the MZF@TiO$_2$ particles. The lower content of titania compared to silica is coherent with the TEM analysis, which showed that MZF@TiO$_2$ particles comprise larger clusters of ferrite crystallites.

FIG. 3 HERE

At the temperature of 5 K, the blocked state of magnetic cores in the bare sample and both the coated products was characterized by hysteresis with similar coercive fields of μ_0H_C = 26–31 mT, whereas negligible coercive fields, μ_0H_C = 1–2 mT, were observed at 300 K. The practically non-hysteretic magnetization curves at room temperature indicate that magnetic cores are superparamagnetic at 300 K while only a negligible component of larger particles persists in the blocked state. This interpretation is confirmed by the ZFC/FC susceptibility studies shown in Fig 4. Both the irreversibility temperature (the bifurcation of the ZFC/FC susceptibility curve) and the distribution of blocking temperatures, inferred from the temperature derivative of the FC and ZFC susceptibility difference, evidence that the studied systems are almost purely superparamagnetic at room temperature.

Further, the ZFC/FC studies revealed a considerable shift of blocking events to lower temperatures upon coating with silica, which can be attributed to suppression of dipolar interactions among ferrite crystallites. TEM showed that magnetic cores of MZF@silica were formed by rather small clusters or just few ferrite crystallites, whose magnetostatic interactions were necessarily confined within individual cores by the thick diamagnetic shell (for the dependence of blocking temperatures on the mean size of clusters see, e.g., [16]). In contrast, the MZF@TiO$_2$ particles comprised larger clusters of ferrite crystallites, and the dipolar interactions among them were comparably important as in the ensemble of bare magnetic particles. Consequently, the distribution of blocking temperatures is similar for MZF@TiO$_2$ and MZF without any obvious effect of the diamagnetic shielding by titania.

FIG. 4 HERE

C. Transverse Relaxivity

The transverse relaxivity, r_2, of coated particles in the

magnetic fields of 0.5 T and 11.75 T is plotted against temperature in Fig. 5a. Both the coated products exhibit high transverse relaxivities compared to traditional contrast agents with iron oxide cores (for a detailed review including r_2 values see, e.g., [17]), possessing thus excellent properties as regards potential applications in MRI. Interestingly, the absolute values and the temperature dependences of r_2 differ significantly for the silica-coated and titania-coated particles.

In order to get a better insight into the variation of r_2 with temperature and to analyze possible role of different relaxation regimes, the temperature dependences of the relaxivity were normalized using their initial values at the lowest temperature and were compared with similarly normalized temperature dependences of selected quantities, namely the self-diffusion coefficient of water, $D(H_2O)$ (calculated based on the Speedy-Angel power-law approach with parameters according to [18]), the magnetization of magnetic cores at 0.5 T, $M(MZF)$, and the expression $M^2(MZF)/D(H_2O)$ (see Fig. 5b). The last quantity models the dependence of r_2 on temperature under the condition of motional averaging regime (MAR) [19]. The dependence observed for MZF@silica particles in both the magnetic fields is a strictly decreasing convex function whose course resembles the temperature dependence of the self-diffusion coefficient of bulk water. This finding indicates that the diffusion of water molecules among whole coated particles strongly affects the transverse relaxivity of MZF@silica by some motional averaging although the experimental data do not comply accurately with the theoretical prediction for MAR.

Surprisingly, the transverse relaxivity of MZF@TiO$_2$ particles is not a monotonic function of temperature. The dependence of r_2 on temperature at 11.75 T is concave and shows a clear maximum between 25 °C and 35 °C. Similar situation is encountered at 0.5 T although the corresponding maximum is less pronounced and is probably shifted to lower temperature. This behavior implies that some thermally activated processes contribute to the dependence of r_2 on temperature because neither MAR nor static dephasing can explain the initial increase of the relaxivity with temperature (not even a mixture of particles in MAR and particles approaching the static dephasing limit with a temperature-dependent ratio of the respective fractions can explain the given observation since the fraction of particles in MAR should increase with temperature). Nevertheless, two clues suggest that titania-coated particles follow rather the static dephasing regime than MAR, namely the high values of r_2 observed for MZF@TiO$_2$ and the comparison of the temperature dependence of r_2 with the theoretical prediction for MAR on one side and the static dephasing limit, where r_2 is proportional to magnetization of particles, on the other side (see Fig. 5b). Finally, the anomalous temperature dependence of r_2 of MZF@TiO$_2$ shows some similarity to the dependence reported recently for La$_{0.65}$Sr$_{0.35}$MnO$_3$ manganite nanoparticles coated with the same mesoporous titania shell [20]. Their transverse relaxivity was lower ($r_2 = 280$ s^{-1}·mmol(La$_{0.65}$Sr$_{0.35}$MnO$_3$) $^{-1}$·L in the magnetic field of 0.5 T and at 20 °C) but exhibited only little variation in the range 5–35 °C while a pronounced decrease of r_2 was observed for their silica-coated counterparts.

FIG. 5 HERE

D. Evaluation of Cytotoxicity

The quantification of viability and proliferation of Jurkat cells by examination of the cell membrane integrity and direct counting of cells is summarized in Fig. 6. Neither the viabilities nor the numbers of cells indicate any toxic effect of both types of coated nanoparticles in the studied range of concentrations (up to 0.14 and 0.07 mmol(Me$_3$O$_4$)·L^{-1} for MZF@silica and MZF@TiO$_2$ particles, respectively), not even after 48 h of the incubation. The values determined were either not significantly different from the negative control or exhibited only small and rather random differences. In contrast, the treatment of Jurkat cells with doxorubicin, a standard chemotherapeutic drug administered intravenously, under the same conditions at the concentration as low as 0.25 µmol·L^{-1} showed dramatic effect on the viability and cell growth. In this case, the viability of 32% was determined 24 h after the treatment, decreasing to only 4% after additional 24 h.

FIG. 6 HERE

To reveal any possible cytotoxic effect of the tested particles, the real-time monitoring of adhesion and proliferation of A549 cells treated with particles was performed. Fig. 7 shows that the cell index is not affected at lower concentrations at all, whereas only a very slight decrease is detected for cells incubated at the highest concentration of particles tested, i.e., 0.14 mmol(Me$_3$O$_4$)·L^{-1} for the silica-coated nanoparticles and 0.07 mmol(Me$_3$O$_4$)·L^{-1} for the titania-coated particles. These observations are consistent with in vitro evaluation of silica-coated MnFe$_2$O$_4$ nanoparticles [21] and confirm the previously reported data on cytotoxicity of comparable silica-coated Mn$_{0.6}$Zn$_{0.4}$Fe$_2$O$_4$ nanoparticles [10]. In contrast, another type of magnetic particles containing manganese, namely silica-coated manganite nanoparticles of the composition La$_{0.63}$Sr$_{0.37}$MnO$_3$ show cytotoxic effects and clear suppression of cell index at concentration as low as 0.055 mmol(La$_{0.63}$Sr$_{0.37}$MnO$_3$)·L^{-1} [10].

FIG. 7 HERE

REFERENCES

[1] Y. Wang and H. C. Gu, "Core-Shell-Type Magnetic Mesoporous Silica Nanocomposites for Bioimaging and Therapeutic Agent Delivery," *Adv. Mater.*, vol. 27, pp. 576-585, Jan 2015.

[2] E. Pollert *et al.*, "Search of new core materials for magnetic fluid hyperthermia: Preliminary chemical and physical issues," *Prog. Solid State Chem.,* vol. 37, no. 1, pp. 1-14, 2009.

[3] J. H. Hankiewicz *et al.*, "Zinc doped copper ferrite particles as temperature sensors for magnetic resonance imaging," *AIP Adv.,* vol. 7, no. 5, 2017, Art. ID 056703.

[4] J. T. Jang *et al.*, "Critical Enhancements of MRI Contrast and Hyperthermic Effects by Dopant-Controlled Magnetic Nanoparticles," *Angew. Chem. Int. Edit.,* vol. 48, no. 7, pp. 1234-1238, 2009.

[5] W. Stöber, A. Fink, and E. Bohn, "Controlled Growth of Monodisperse Silica Spheres in the Micron Size Range," *J. Colloid Interface Sci.*, vol. 26, pp. 62-69, 1968.

[6] A. P. Philipse, M. P. B. van Bruggen, and C. Pathmamanoharan, "Magnetic silica dispersions: preparation and stability of surface-modified silica particles with a magnetic core," *Langmuir*, vol. 10, pp. 92-99, Jan. 1994.

[7] F. U. Rehman, C. Zhao, H. Jiang, and X. Wang, "Biomedical applications of nano-titania in theranostics and photodynamic therapy," *Biomater. Sci.,* vol. 4, no. 1, pp. 40-54, 2016.

[8] A. Jańczyk, E. Krakowska, G. Stochel, and W. Macyk, "Singlet Oxygen Photogeneration at Surface Modified Titanium Dioxide," *J. Am. Chem. Soc.*, vol. 128, pp. 15574-15575, Dec. 2006.

[9] O. Kaman *et al.*, "Preparation of Mn-Zn ferrite nanoparticles and their silica-coated clusters: Magnetic properties and transverse relaxivity," *J. Magn. Magn. Mater.,* vol. 427, pp. 251-257, Apr. 2017.

[10] O. Kaman *et al.*, "Silica-coated manganite and Mn-based ferrite nanoparticles: a comparative study focused on cytotoxicity," *J. Nanopart. Res.,* vol. 18, no. 4, Apr. 2016, Art. ID 056703.

[11] B. E. Yoldas, "Hydrolysis of titanium alkoxide and effects of hydrolytic polycondensation parameters," *J. Mater. Sci.,* vol. 21, pp. 1087-1092, Mar. 1986.

[12] G. D. Panagiotou *et al.*, "Mapping the surface (hydr)oxo-groups of titanium oxide and its interface with an aqueous solution: The state of the art and a new approach," *Adv. Colloid Interface Sci.,* vol. 142, pp. 20-42, Oct. 2008.

[13] R. I. Nooney, D. Thirunavukkarasu, Y. M. Chen, R. Josephs, and A. E. Ostafin, "Synthesis of nanoscale mesoporous silica spheres with controlled particle size," *Chem. Mat.,* vol. 14, pp. 4721-4728, Nov. 2002.

[14] T. Peng, D. Zhao, K. Dai, W. Shi, and K. Hirao, "Synthesis of Titanium Dioxide Nanoparticles with Mesoporous Anatase Wall and High Photocatalytic Activity," *J. Phys. Chem. B,* vol. 109, pp. 4947-4952, Mar. 2005.

[15] C. Rath, S. Anand, R. P. Das, K. K. Sahu, S. D. Kulkarni, S. K. Date, and N. C. Mishra, "Dependence on cation distribution of particle size, lattice parameter, and magnetic properties in nanosize Mn-Zn ferrite," *J. Appl. Phys.*, vol. 91, pp. 2211-2215, Feb. 2002.

[16] T. Dědourková *et al.*, "Clusters of magnetic nanoparticles as contrast agents for MRI: the effect of aggregation on transverse relaxivity," *IEEE Trans. Magn.,* vol. 51, no. 11, Nov. 2015, Art. ID 5300804.

[17] S. Laurent *et al.*, "Magnetic Iron Oxide Nanoparticles: Synthesis, Stabilization, Vectorization, Physicochemical Characterizations, and Biological Applications," *Chem. Rev.,* vol. 108, pp. 2064-2110, Jun. 2008.

[18] M. Holz, S. R. Heil, and A. Sacco, "Temperature-dependent self-diffusion coefficients of water and six selected molecular liquids for calibration in accurate ^{1}H NMR PFG measurements," *Phys. Chem. Chem. Phys.,* vol. 2, no. 20, pp. 4740-4742, 2000.

[19] M. R. J. Carroll *et al.*, "Experimental validation of proton transverse relaxivity models for superparamagnetic nanoparticle MRI contrast agents," *Nanotechnology,* vol. 21, Jan. 2010, Art. ID 035103.

[20] Z. Jirák, J. Kuličková, V. Herynek, M. Maryško, J. Koktan, and O. Kaman, "Titania-coated manganite nanoparticles: Synthesis of the shell, characterization and MRI properties," *J. Magn. Magn. Mater.*, vol. 427, pp. 245-250, Apr. 2017.

[21] B. Sahoo, K.S.P. Devi, S. Dutta, T.K. Maiti, P. Pramanik, D. Dhara, "Biocompatible mesoporous silica-coated superparamagnetic manganese ferrite nanoparticles for targeted drug delivery and MR imaging applications," *J. Colloid Interface Sci.*, vol. 431, 3-41, Oct. 2014.
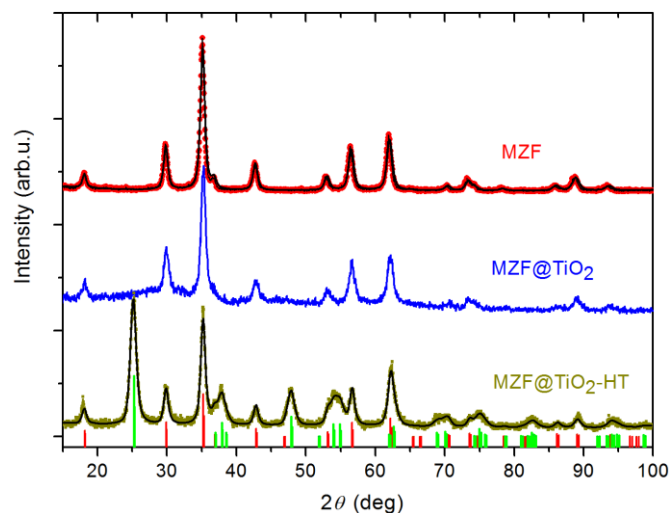
Fig. 1. XRD patterns of bare ferrite nanoparticles (MZF), as-prepared titania-coated product (MZF@TiO$_2$), and the titania-coated sample after the hydrothermal treatment at 200 °C (MZF@TiO$_2$-HT). The red vertical bars indicate diffractions of the spinel phase of the $Fd\bar{3}m$ symmetry, whereas the green bars show diffraction lines of the anatase with the $I4_1/amd$ symmetry.
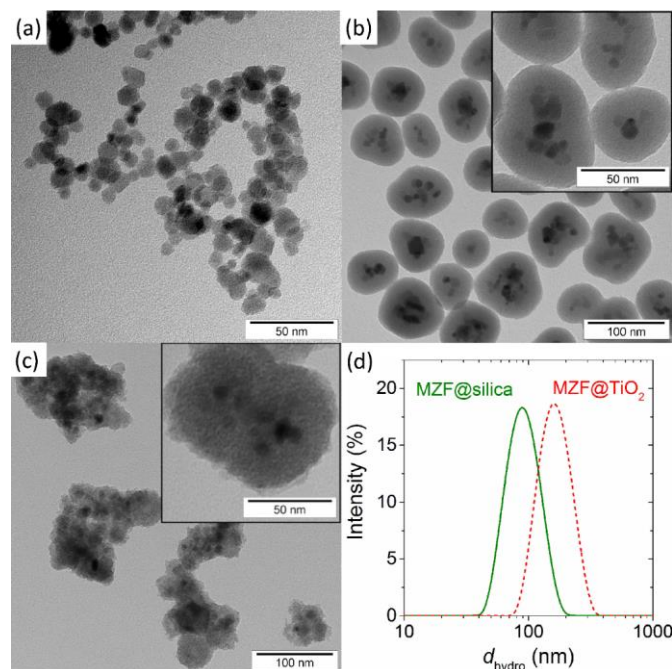

Fig. 2. TEM and DLS studies of the prepared samples: (a) bare Mn$_{0.61}$Zn$_{0.42}$Fe$_{1.97}$O$_4$ nanoparticles stabilized by citrate, (b) silica-coated product, (c) titania-coated sample, (d) the intensity distribution of hydrodynamic size, d_{hydro}, for both the coated samples in water.
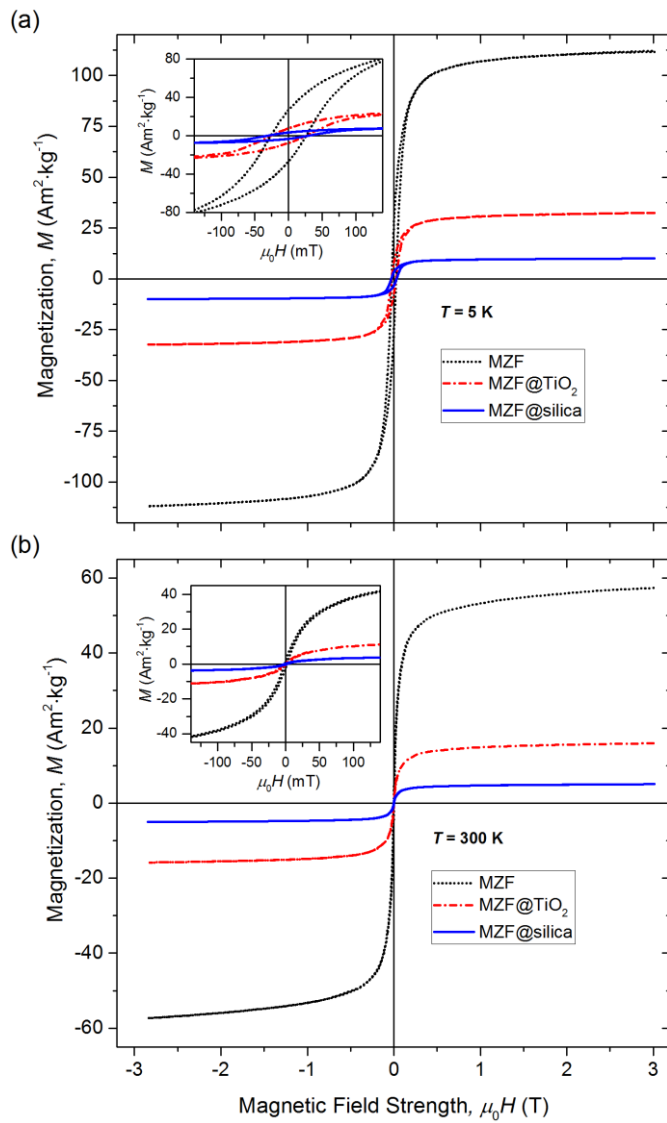
Fig. 3. Hysteresis loops of bare, silica-coated, and titania-coated $Mn_{0.61}Zn_{0.42}Fe_{1.97}O_4$ nanoparticles at low (a) and room (b) temperatures.
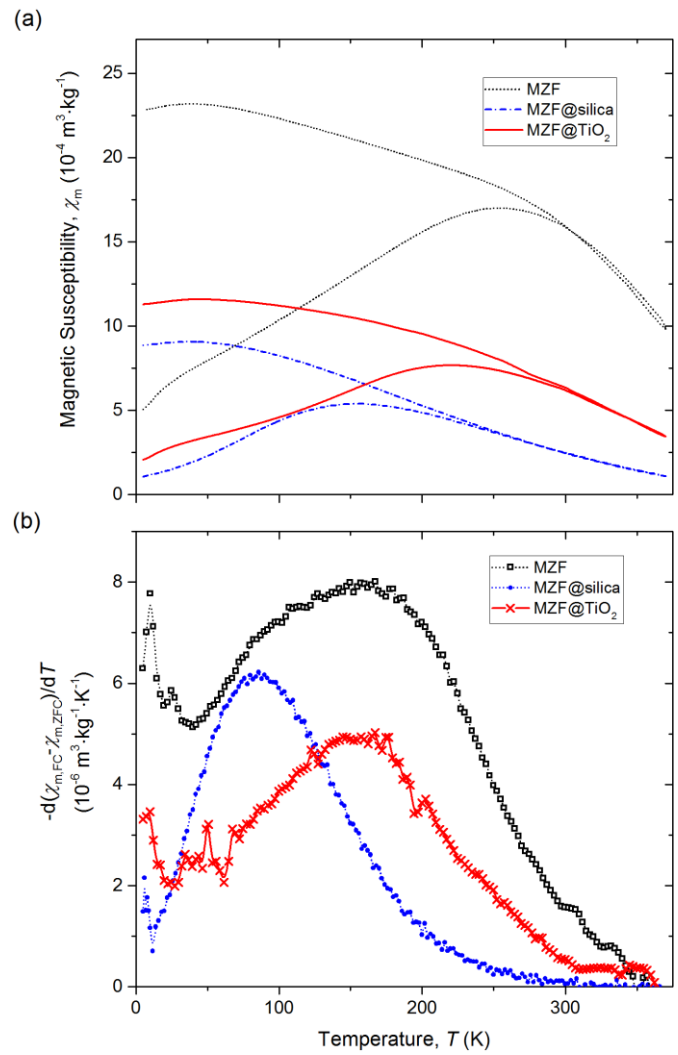

Fig. 4. ZFC-FC measurements in the magnetic field of $H = 1.59$ kA·m^{-1}: (a) ZFC and FC susceptibilities, $\chi_{m,ZFC}$ and $\chi_{m,FC}$, (b) temperature derivative of the $\chi_{m,FC}$-$\chi_{m,ZFC}$ difference.
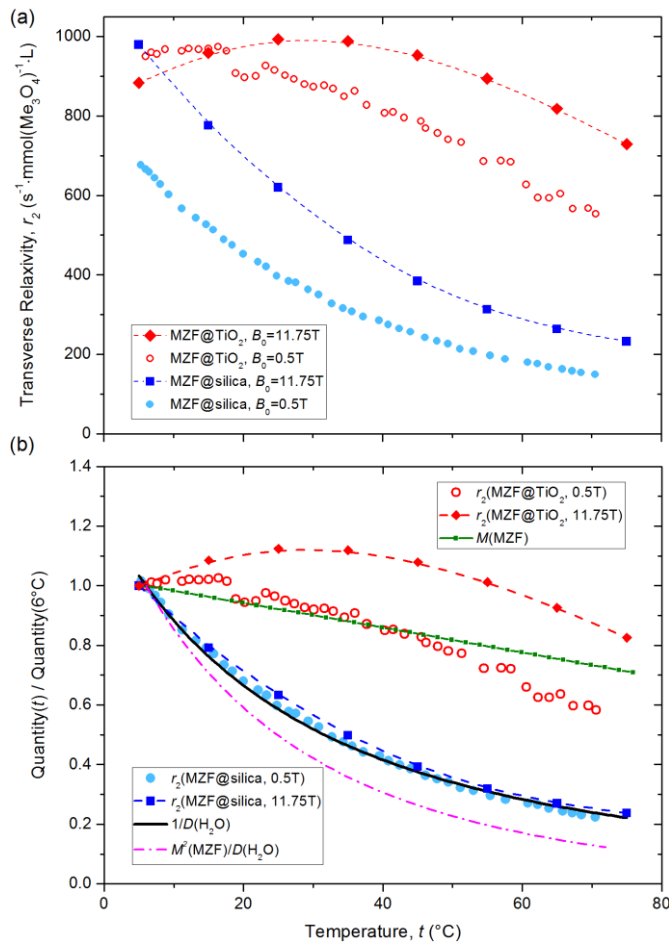
Fig. 5. Relaxometric study: (a) temperature dependence of the transverse relaxivity, r_2, for silica-coated and titania-coated $Mn_{0.61}Zn_{0.42}Fe_{1.97}O_4$ nanoparticles in magnetic fields of $B_0 = 0.5$ T and 11.75 T; (b) comparison of the temperature dependence of r_2 with the inverse value of the self-diffusion coefficient of water, $1/D(H_2O)$, the magnetization of bare ferrite particles at 0.5 T, $M(MZF)$, and the expression $M^2(MZF)/D(H_2O)$, which describes the motional averaging regime. All the quantities are normalized using their values at the temperature of $t = 6$ °C.
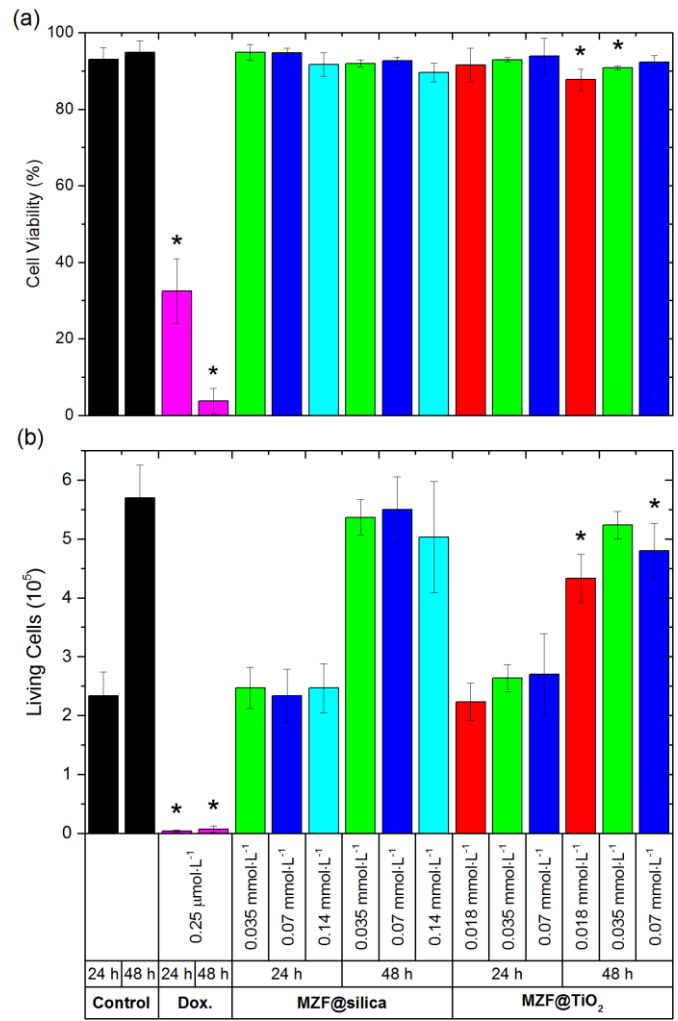

Fig. 6. The effect of silica-coated and titania-coated $Mn_{0.61}Zn_{0.42}Fe_{1.97}O_4$ nanoparticles on the viability (a) and proliferation (b) of Jurkat cells. The cells treated with doxorubicin (Dox.) at the concentration of 0.25 μmol(Me$_3$O$_4$)·L^{-1} and the cells treated with sterile deionized water were used as positive and negative controls, respectively. The concentration of coated particles is expressed as the molar concentration of formula units, i.e., Me$_3$O$_4$, and the results are shown as mean values ± standard deviations. Asterisk indicates values significantly different to the negative control on the significance level of 5%.
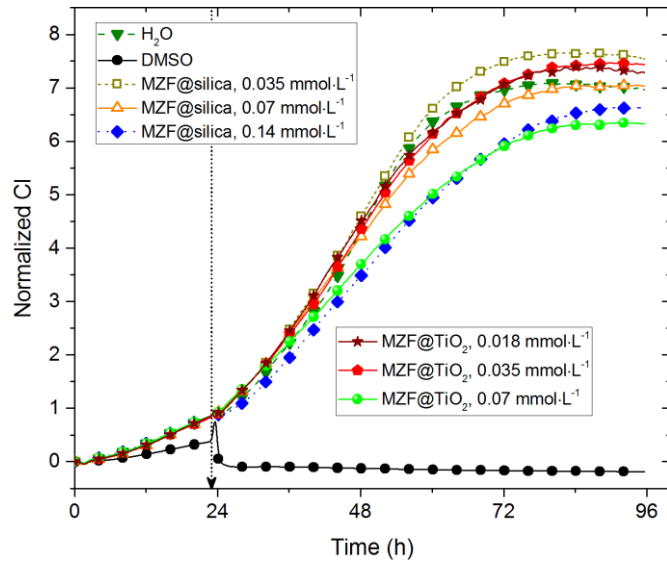
Fig. 7. Real-time monitoring of adhesion and proliferation of A549 cells by the xCELLigence system. The cells were treated with silica-coated and titania-coated $Mn_{0.61}Zn_{0.42}Fe_{1.97}O_4$ nanoparticles at three different concentrations (expressed as the molar concentration of formula units, i.e., Me_3O_4), and the cell index, CI, was recorded as a function of time. The cells treated with sterile deionized water were used as negative control, whereas cells treated with 5% DMSO were employed as positive control.